



Broadband gigahertz dynamics of relaxor ferroelectric $\text{Pb}(\text{Sc}_{1/2}\text{Nb}_{1/2})\text{O}_3-x\text{PbTiO}_3$ single crystal probed by Brillouin scattering

著者	Kojima S., Tsukada S., Hidaka Y., Bokov A. A., Ye Z.-G.
journal or publication title	Journal of applied physics
volume	109
number	8
page range	084114
year	2011-04
権利	Copyright 2011 American Institute of Physics. This article may be downloaded for personal use only. Any other use requires prior permission of the author and the American Institute of Physics. The following article appeared in J. Appl. Phys. 109, 084114 and may be found at http://jap.aip.org/resource/1/japiau/v109/i8/p084114_s1 .
URL	http://hdl.handle.net/2241/113331

doi: 10.1063/1.3581025

Broadband gigahertz dynamics of relaxor ferroelectric $\text{Pb}(\text{Sc}_{1/2}\text{Nb}_{1/2})\text{O}_3$ - $x\text{PbTiO}_3$ single crystal probed by Brillouin scattering

S. Kojima,^{1,a)} S. Tsukada,^{1,b)} Y. Hidaka,¹ A. A. Bokov,² and Z.-G. Ye^{2,c)}¹Graduate School of Pure and Applied Sciences, University of Tsukuba, Tsukuba, Ibaraki 305-8573, Japan²Department of Chemistry & 4D LABS, Simon Fraser University, Burnaby, British Columbia V5A 1S6, Canada

(Received 14 January 2011; accepted 12 March 2011; published online 26 April 2011)

The broadband gigahertz dynamics of a relaxor ferroelectric crystal $0.70\text{Pb}(\text{Sc}_{1/2}\text{Nb}_{1/2})\text{O}_3$ - 0.30PbTiO_3 with a composition close to the starting point of the morphotropic phase boundary is studied by Brillouin scattering. The significant anomaly of the longitudinal acoustic (LA) mode is observed in the vicinity of the Curie temperature, $T_C = 500$ K. Upon cooling, it starts below the Burns temperature, $T_B = 670$ K, due to the interaction between the LA mode and dynamic polar nanoregions (PNRs). The broad central peak (CP) clearly appears below T_B , and its intensity becomes a maximum at T_C . The relaxation time, τ_{CP} , determined from the CP width, shows the typical critical slowing down of the order-disorder phase transition in the vicinity of T_C . The size of a dynamic PNR significantly increases below the intermediate temperature, $T^* = 562$ K.

© 2011 American Institute of Physics. [doi:10.1063/1.3581025]

I. INTRODUCTION

Relaxor ferroelectric-based solid solution single crystals have attracted much attention because of the giant piezoelectricity and high electromechanical coupling factor.¹ Relaxor ferroelectrics exhibit a broad and large maximum of dielectric constant at the temperature, T_m , around which a pronounced dielectric dispersion appears. It has been extensively discussed and commonly agreed that the static chemically ordered regions (CORs) and the polar nanoregions (PNRs) play an important role in the appearance of the relaxor behavior.²⁻⁴ However, recent studies have shown that the CORs do not contribute to the relaxation dynamics of relaxors.^{5,6} It is confirmed that the dynamic PNRs appear below the Burns temperature, T_B ,⁷ but the microscopic mechanism underlying their appearance, growth, dynamics, and length scale are still unclear.

Due to the colossal piezoelectric effect, the polarization fluctuations induce the colossal strain fluctuations, which interact with the long wavelength acoustic waves. Recent observation of the acoustic emission (AE) of Pb-based relaxors at the intermediate temperature, T^* , between T_B and T_m suggests that the rapid growth in the size of PNRs generates AE bursts.⁸ Such acoustic waves are detectable by a conventional ultrasonic transducer in the kilohertz to the megahertz range. In contrast, the Brillouin scattering technique detects the acoustic modes in the gigahertz range the wave length of which is much shorter than that of the standard ultrasonic detection.

Therefore the temperature variation of local polarization fluctuations of the PNRs can be more sensitively detected by

the broadband Brillouin scattering technique in the frequency range from 1 to 1000 GHz.⁹ Svitelskiy *et al.* also proposed the existence of an intermediate temperature on the basis of a Raman spectra analysis in the terahertz range.¹⁰

In $\text{Pb}(\text{B}'_{1/2}\text{B}''_{1/2})\text{O}_3$ -type relaxors, the degree of cation ordering at the B-site can depend on the heat treatment at high temperatures. A well-annealed sample of B-site ordered $\text{Pb}(\text{Sc}_{1/2}\text{Nb}_{1/2})\text{O}_3$ (PSN), $\text{Pb}(\text{Sc}_{1/2}\text{Ta}_{1/2})\text{O}_3$ (PST) undergoes a normal ferroelectric transition, whereas a quenched one with a B-site disorder shows the relaxor nature.^{11,12} Upon cooling from high temperatures, disordered PSN (PSN-*D*) first enters an ergodic relaxor state and then spontaneously transforms into a ferroelectric phase at the Curie temperature, T_C , substantially below T_m .¹³ A recent Brillouin scattering study showed the order-disorder nature of the PSN-*D* in the vicinity of $T_C = 373$ K.¹⁴ It was also found that the relaxor state in the PSN-*D* can be suppressed by the hydrostatic pressure and a DC electric field.¹⁵⁻¹⁸ For the $(1-x)\text{Pb}(\text{Sc}_{1/2}\text{Nb}_{1/2})\text{O}_3$ - $x\text{PbTiO}_3$ (PSN-100xPT) solid solution, the schematic phase diagram of the PSN-PT is shown in Fig. 1.¹⁹⁻²⁵ Besides, the composition dependence of the ferroelectric phase transition enthalpy has the minimum around $x = 0.30$ with the composition close to the starting point of MPB, which means that in this composition a phase transition is comparatively a second order.¹⁹ In the present study, the broadband Brillouin scattering of a PSN-30PT ($x = 0.30$) single crystal was investigated to provide new insights into the PNRs related to the nanoscale dynamic heterogeneity.

II. EXPERIMENTAL

The PSN-30PT single crystals were grown by the high temperature solution method at Simon Fraser University.²³ The specimen was cut having the size of $1.5 \times 1.5 \times 0.2$ mm³ with the largest faces oriented perpendicular to the

^{a)}Electronic mail: kojima@bk.tsukuba.ac.jp.^{b)}Present address: Faculty of Education, Shimane University, Matsue 690-8504, Japan.^{c)}Electronic mail: zye@sfu.ca.

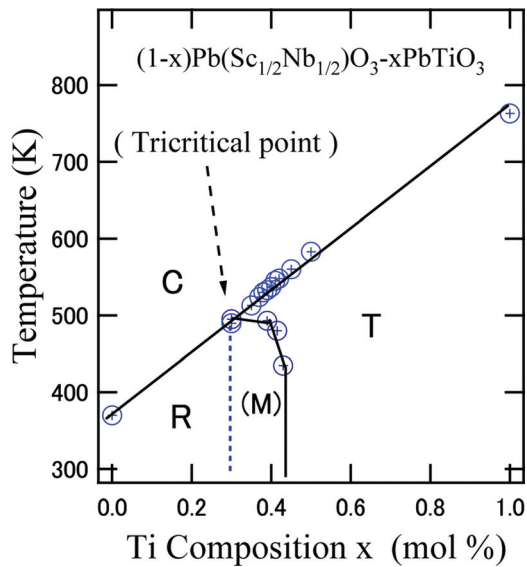


FIG. 1. (Color online) Schematic phase diagram of $(1-x)\text{Pb}(\text{Sc}_{1/2}\text{Nb}_{1/2})\text{O}_3-x\text{PbTiO}_3$ using the reported values from Refs. 19–25. The starting point of the MPB may be close to a tricritical point.

pseudocubic [100] direction. The two (100) faces were polished to an optical grade. The Brillouin scattering was measured by a micro-Brillouin scattering apparatus, which is a combination of a microscope and a Sandercock-type 3 + 3 passes tandem multipass Fabry—Perot interferometer at University of Tsukuba.²⁶ All spectra were measured at a backward scattering geometry. The objective lens of the microscope focuses an incident laser beam onto the sample and simultaneously collects the scattered light to be studied. An ordinary photon counting system and a multi-channel analyzer were used to accumulate the output signals. The temperature was controlled by the heating and cooling stage of a THMS 600 temperature controller (Linkam) from 90 to 870 K. The temperature stability of a sample was within ± 0.1 K over the entire temperature range.

III. RESULTS AND DISCUSSION

A. Elastic anomaly

To study the elastic anomaly in the vicinity of $T_C = 500$ K, the temperature dependence of the Brillouin scattering spectra was measured above and below T_C . Figure 2(a) shows the broadband Brillouin scattering spectra at three temperatures. The broad peak at 0 GHz is a central peak (CP), and sharp peaks at about 33 and 46 GHz at 493 K are transverse acoustic (TA) and LA peaks, respectively. The change of LA peaks is clearly observed in the spectra of narrow frequency range as shown in Fig. 2(b). For the fitting of CP, which is related to polarization fluctuations, the distribution of relaxation time may appear near T_C , while we assume the Debye relaxation to avoid the ambiguity caused by increase of the number of fitting parameters. For the fitting of a LA peak, because the peak width is relatively small, a Lorentzian function is a good approximation of a damped harmonic oscillator model. Therefore, in Figs. 2(a) and 2(b), solid lines for CP, TA, and LA peaks are the fitted curves by three Lorentzian functions. The temperature dependence of

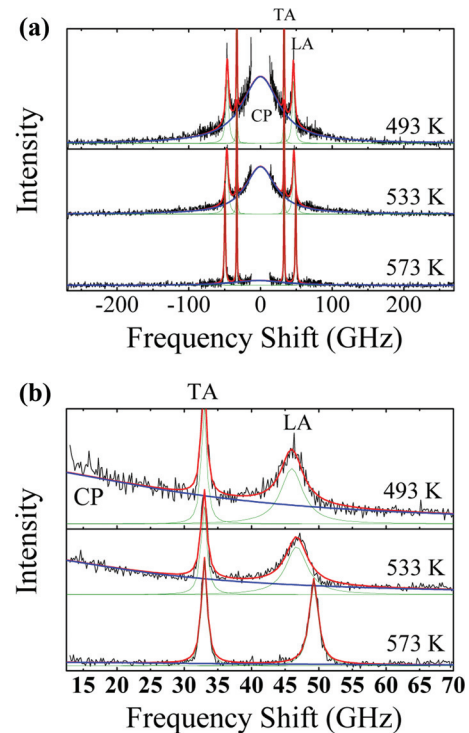


FIG. 2. (Color online) (a) The broadband Brillouin scattering spectra of a PSN-30PT crystal at three temperatures. The broad peak at 0 GHz is CP and sharp peaks at about 33 and 46 GHz at 493 K are TA and LA peaks, respectively. (b) In the spectra of narrow frequency range, the change of LA peaks is clearly observed.

the TA mode is not discussed in this paper because the temperature range for the appearance of the TA peaks is limited. The temperature dependence of the Brillouin shift of the LA mode, which is proportional to the LA phase velocity, is shown in Fig. 3. Upon cooling, the shift shows a remarkable softening due to the interaction between the LA mode and the polarization flippings inside the dynamic PNRs.^{8,9} In Fig. 3, the frequency shifts of a PSN-D single crystal¹⁴ are

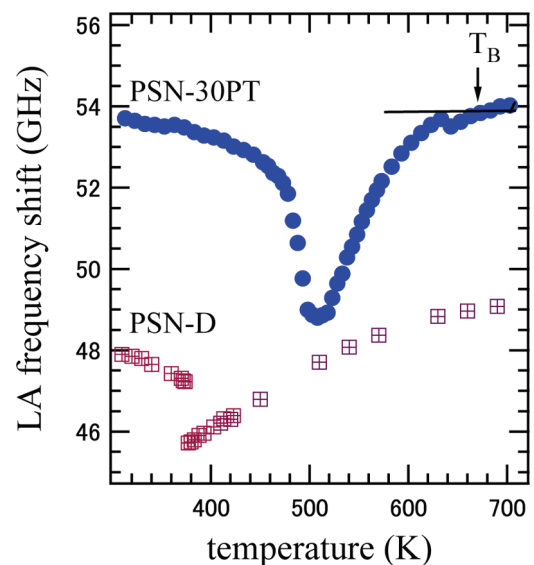


FIG. 3. (Color online) Temperature dependence of the LA frequency shift of a PSN-30PT crystal. The result of a PSN-D crystal from Ref. 14 is also plotted for comparison.

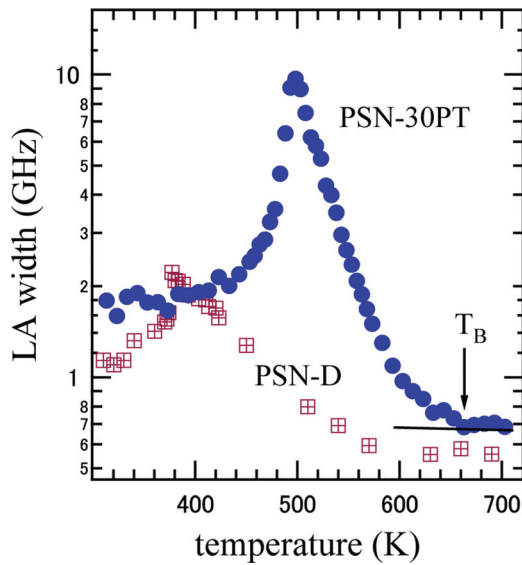


FIG. 4. (Color online) Temperature dependence of the LA peak width of a PSN-30PT crystal upon cooling gives $T_B = 670$ K. The result of a PSN-D crystal from Ref. 14 is also plotted for comparison. The onset of the increase in the peak width upon cooling gives $T_B = 670$ K.

also plotted for comparison. The elastic anomaly near T_C of the PSN-D is much smaller than that of the PSN-PT, and it indicates that the ferroelectric phase transition of the PSN-D is of the typical first order nature.

The LA peak width is plotted as a function of temperature as shown in Fig. 4. Upon cooling, the LA width significantly increases toward T_C due to the increase in the attenuation by the interaction with the dynamic PNRs. Such an elastic anomaly is very common in relaxor ferroelectrics.^{8,9} The temperature dependence of the LA width of PSN-D¹⁴ is also plotted in Fig. 4 for the comparison. A nearly divergent increase in the damping is observed at T_C in the PSN-30PT, while the increased damping of the PSN-D is much smaller. These results regarding the LA frequency shift and damping indicate that the phase transition in the PSN-30PT becomes nearly second order in comparison with that of the PSN-D in agreement with the previous calorimetric measurement.¹⁹ This fact can be related to the enhancement of piezoelectric effect near the MPB composition starting from a tricritical point (TCP) as observed in the BZT-BCT.²⁷ This scenario might occur also in PSN-xPT; this would explain the enhancement of critical slowing down near TCP from which the MPB starts as shown in Fig. 1.

B. Critical slowing down

The relaxation process related to the order-disorder nature in a ferroelectric phase transition has been observed as a central peak (CP) around zero frequency shift in an inelastic scattering spectrum.^{28,29} The Brillouin scattering spectra of the PSN-30PT clearly showed a broad CP below and above T_C as shown in Fig. 2. Under the assumption of a single Debye relaxation process, the relaxation time τ_{CP} is determined by the relation $\pi \times (\text{CP width}) \times \tau_{CP} = 1$. The temperature dependence of the inverse τ_{CP} is plotted in Fig. 5. It

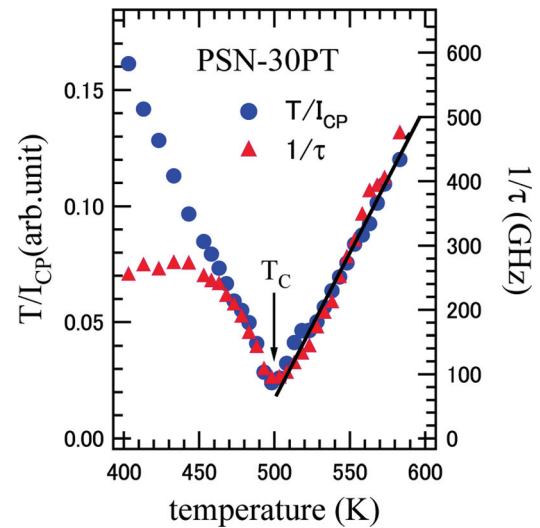


FIG. 5. (Color online) Temperature dependence of the inverse relaxation time and T/I_{CP} of a PSN-30PT crystal.

was found that the critical slowing down given by Eq. (1) is clearly observed above $T_C = 500$ K.

$$\frac{1}{\tau_{CP}} = \frac{1}{\tau_0} + \frac{T - T_C}{\tau_1 T_C}, \quad \text{for } T > T_C, \quad (1)$$

where $\tau_0 = 14$ ps and $\tau_1 = 0.47$ ps are the fitting parameters. Below T_C , in the narrow temperature interval of 470-500 K, the inverse relaxation time approximately follows Eq. (1) as expected in a second-order phase transition. However, a deviation is observed below T_C because the distribution of the relaxation time appears due to domain wall dynamics. As to the $\text{Pb}(\text{B}'_{1/2}\text{B}''_{1/2})\text{O}_3$ -type relaxors, in addition to PSN-D (Ref. 14), the ferroelectric transition of the $0.65\text{Pb}(\text{In}_{1/2}\text{Nb}_{1/2})\text{O}_3$ - 0.35PbTiO_3 (PIN-35PT) crystal show also the order-disorder nature above $T_C \sim 540$ K.³⁰

The observed critical slowing down is characteristic of normal order-disorder type ferroelectric,³¹ and up to the present it has not been observed in the canonical relaxors such as the PMN. For the $\text{Pb}(\text{B}'_{1/2}\text{B}''_{1/2})\text{O}_3$ -type relaxors such as the PSN and the PIN-35PT, it has been only recently discovered,^{14,30} therefore it requires a more detailed discussion. In normal ferroelectrics, in which the permanent dipole moments in a paraelectric phase (that is, at $T > T_C$) can be associated with the unit cells, whereas on the large scale, the structure is nonpolar. In contrast, upon cooling the relaxors do not directly transform (at T_B) from a paraelectric phase to a ferroelectric one but to an “ergodic relaxor” phase.⁴ In the ergodic relaxor phase, the PNRs exist (several nonometers in size) in which the dipole moments of the unit cells are *permanently* ordered in a ferroelectric manner. The main relaxation process in this phase is related to the reorientation (flipping) of the dipole moments of the PNRs (in other words, simultaneous reorientations of unit cells inside a particular PNR).

In a canonical relaxors, such as the PMN or the La-doped $\text{Pb}(\text{Zr}_{1-x}\text{Ti}_x)\text{O}_3$, the random fields and the frustrated interactions among PNRs lead to the non-Arrhenius

slowing down of their relaxation time. Upon further cooling, they transform into the glassy “nonergodic relaxor” state in which the PNR dipole moments are randomly frozen in different directions so that the crystal remains mesoscopically isotropic. The mean relaxation of this process follows the Vogel—Fulcher-type temperature dependence in which the relaxation time becomes very long and inaccessible for the high frequency range of the Brillouin scattering technique except for high temperatures. Accordingly the relaxation time derived from the CP width represents the lower edge of the wide spectrum of the relaxation time distribution and show a weak nondivergent temperature dependence.³² However, in the $\text{Pb}(\text{B}'_{1/2}\text{B}''_{1/2})\text{O}_3$ -type relaxors [including the PSN, the PIN-35PT (Ref. 30) and the PSN-30PT studied in this work], the transition from the ergodic relaxor to the ferroelectric phase is observed instead of the glassy freezing. This variation in behavior can be attributed (at least in some case) to the different mode of interactions among the PNRs, namely, the interactions promote the ordering of the PNRs dipole moments in the unique direction and induce the order-disorder type ferroelectric phase transition at T_C . In this case, the PNRs with their “giant” dipole moments play the same role as do the cooperative polar molecules in normal order-disorder type ferroelectrics. From this analogy, one may expect that the relaxation time of the PNR flipping diverges at (or close to) T_C following Eq. (1) as we have indeed observed. Close to the temperature of a second-order phase transition, one can expect a large fluctuations in the order-disorder-type polarizations (that is, the regions where the dipole moments of many PNRs are ferroelectrically ordered). These fluctuations increase the CP intensity and couple to the LA phonons, giving rise to their additional softening.

Next we discuss the result that the CP intensity becomes a maximum at T_C . In the high temperature approximation, the quantity of the temperature divided by the CP intensity T/I_{CP} is proportional to the real part of the inverse dynamic susceptibility $\chi'(0)$ of the low-frequency limit of Brillouin scattering.²⁸

$$\frac{T}{I_{CP}} \propto \left[\int_0^{\infty} \frac{\chi''(\omega)}{\omega} d\omega \right]^{-1} \propto \chi'(0)^{-1}. \quad (2)$$

The origin of CP in the Pb-based relaxors is the polarization flippings inside the dynamic PNRs.^{9,26,28} Such polar motions are infrared active, therefore the dynamic susceptibility is related to the dielectric susceptibility, which may obey the extended Curie-Weiss law

$$\frac{1}{\chi'(0)} = \frac{1}{\chi_b} + \frac{(T-T_C)^\gamma}{2\delta^2}, \quad (3)$$

where χ_b , γ , and δ are the fitting parameters. Fig. 5 shows the temperature dependence of the T/I_{CP} , which is found to obey the case of $\gamma=1$ of Eq. (3) above T_C . Because, $\chi'(0)$ is the susceptibility of the low-frequency limit of Brillouin scattering measurements, the value of γ may increase for the dielectric constant of the kilohertz frequency range measured by the conventional impedance analyzer.

C. Size of dynamic PNR

The density fluctuations on a nanometer scale play a dominant role in the precursor phenomena during a martensitic transformation, liquid-glass transition, etc. In an austenite phase, premartensitic embryos appear, and in a supercooled liquid, the strain relaxation on a nanometer scale has been extensively discussed regarding the density fluctuation using the term of the nanoscale strain relaxing region, which is defined by the products of sound velocity and relaxation time.³³ The characteristic length of such a relaxing region is closely related to the classical idea of a cooperative rearrangement region (CRR) on a nanometer scale in which the molecular motion is cooperative.³⁴ In relaxors, dynamic PNRs play the dominant role in the high frequency local dynamics on a nanometer length scale. In this section, we discuss the size of a dynamic PNR in a way similar to the dynamics of a CRR. The thermally fluctuating flipping of the local spontaneous polarization inside a particular PNR induces flipping of local strain inside a PNR through the colossal piezoelectric coupling due to the polar symmetry inside a PNR. The analysis of the 180° flipping of the local polarization inside a PNR shows the existence of density fluctuations of PNRs.⁹ In the neutron inelastic scattering studies, a strong coupling was reported between the TA mode with a nanometer wavelength and PNRs,³⁵ whereas, in a long wavelength acoustic mode of a few hundred nanometers, the LA mode essentially couples to the dynamics of PNRs. During the flipping of local polarizations inside a PNR, which couples to the local strain flipping inside a PNR, the speed of the propagation of strain flipping motion can be the phase velocity of the LA mode. Therefore the size of a flipping PNR is approximately equal to the propagation length of the LA mode during the flipping period, which is given by the product of the LA velocity V_{LA} and the relaxation time τ_{CP} . Consequently, this length, $l_{PNR} = V_{LA} \times \tau_{CP}$, may give the rough estimation of the size of a dynamic PNR.^{26,36}

The size of a dynamic PNR, l_{PNR} , is calculated from the CP width and the LA frequency shift. Figure 6 shows the

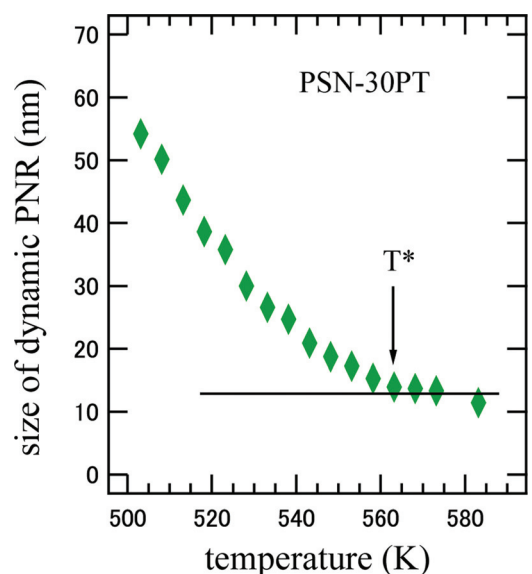


FIG. 6. (Color online) Temperature dependence of the size of a dynamic PNR of a PSN-30PT crystal.

temperature dependence of l_{PNR} . Above $T^* = 562$ K, the size of a dynamic PNR is nearly constant because PNRs only dynamically fluctuate and their size does not grow. Whereas below T^* , the size of a dynamic PNR shows a significant increase below T^* as shown in Fig. 6. The value of the size of 14 nm at T^* gives presumably the initial size of a dynamic PNR to grow, and above this value, a dynamic PNR increases in size and changes into a slower or static PNR. In the $(1-x)\text{Pb}(\text{Zn}_{1/3}\text{Nb}_{2/3})\text{O}_{3-x}\text{PbTiO}_3$ (PZN-100xPT), the AE study reported the intermediate temperature of $T^* \sim 500$ K.⁸ In PZN-7PT,³⁶ the initial size about 2.5 nm at T^* is much smaller than that of PSN-30PT, and the slowing down of the relaxation time is suppressed as similar as the case of the PMN.³⁶ Such a difference of the growing process of dynamic PNRs reflects the difference of frustrations between $\text{Pb}(\text{B}'_{1/2}\text{B}''_{1/2})\text{O}_3$ -type and $\text{Pb}(\text{B}'_{1/3}\text{B}''_{2/3})\text{O}_3$ -type relaxors.³⁵ Even though the quasistatic or static long range order appears for further cooling, the size of a dynamic PNR estimated by Brillouin scattering does not diverge at T_C because the Brillouin scattering measurements cannot detect the slower flipping below the gigahertz range.

IV. CONCLUSION

The ferroelectric phase transition of the relaxor ferroelectric PSN-30PT crystal with a composition close to the starting point of MPB was studied by Brillouin scattering. Although the weak elastic anomaly of the PSN- D near $T_C = 373$ K shows a first order nature,¹⁴ the PSN-30PT exhibits a remarkable elastic anomaly near $T_C = 500$ K; this is reminiscent of the critical behavior of a second-order phase transition. Upon cooling, the width of the LA mode begins to increase below the Burns temperature, $T_B = 670$ K. The broad CP clearly appears below T_B , and its intensity shows the significant increase in the vicinity of T_C , reflecting the growth of dynamic PNRs. The relaxation time τ_{CP} shows the critical slowing down of the order-disorder nature in the vicinity of T_C . This fact suggests that the ferroelectric phase transition of the PSN-30PT with the starting composition of MPB is close to a second-order phase transition. It was found that the size of a dynamic PNR starts to increase at the intermediate temperature, $T^* = 562$ K, indicating a rapid growth of a dynamic PNR occurring below T^* .

ACKNOWLEDGMENTS

The authors are thankful to Dr. Y. Bing for help with the crystal growth. This work is supported in part by the Grant-in-Aids from MEXT, Japan for University of Tsukuba, and

the U. S. Office of the Naval Research (Grant No. N00014-06-1-0166) and Natural Science & Engineering Research Council of Canada for Simon Fraser University.

- ¹Z.-G. Ye, *Mater. Res. Soc. Bull.* **34**, 277 (2009).
- ²G. A. Smolenskii, *J. Phys. Soc. Jpn.* **28**, Suppl. 26 (1970).
- ³L. E. Cross, *Ferroelectrics* **76**, 241 (1987).
- ⁴A. A. Bokov and Z.-G. Ye, *J. Mater. Sci.* **41**, 31 (2006).
- ⁵X. Zhao, W. Qu, X. Tan, A.A. Bokov, and Z.-G. Ye, *Phys. Rev. B* **79**, 144101 (2009).
- ⁶S. Kamba, D. Nuzhnyy, S. Velijko, V. Bovtun, J. Petzelt, Y. L. Wang, N. Setter, J. Levoska, M. Tyunina, J. Macutkevicius, and J. Banys, *J. Appl. Phys.* **102**, 074106 (2007).
- ⁷G. Burns and F. H. Dacol, *Solid State Commun.* **28**, 853 (1983).
- ⁸M. Roth, E. Mojaev, E. Dul'kin, P. Gemeiner, and B. Dkhil, *Phys. Rev. Lett.* **98**, 265701 (2007).
- ⁹S. Tsukada and S. Kojima, *Phys. Rev. B* **78**, 144106 (2008).
- ¹⁰O. Svitelskiy, J. Toulouse, G. Yong, and Z.-G. Ye, *Phys. Rev. B* **68**, 104107 (2003).
- ¹¹F. Chu, I. M. Reaney, and N. Setter, *J. Appl. Phys.* **77**, 1671 (1995).
- ¹²C. G. F. Stenger and A. J. Burggraaf, *Phys. Stat. Solidi A* **61**, 275 (1980).
- ¹³G. A. Samara, *Phys. Rev. B* **71**, 224108 (2005).
- ¹⁴M. Ahart, A. Hushur, Y. Bing, Z.-G. Ye, R. J. Hemley, and S. Kojima, *Appl. Phys. Lett.* **94**, 142906 (2009).
- ¹⁵E. L. Venturini, R. K. Grubbs, G. A. Samara, Y. Bing, and Z.-G. Ye, *Phys. Rev. B* **74**, 064108 (2006).
- ¹⁶P. Ganesh, E. Cockayne, M. Ahart, R. E. Cohen, B. Burton, R. J. Hemley, Y. Ren, W. Yang, and Z.-G. Ye, *Phys. Rev. B* **81**, 144102 (2010).
- ¹⁷M. Ahart, H. Mao, R. E. Cohen, R. J. Hemley, G. A. Samara, Z.-G. Ye, and S. Kojima, *J. Appl. Phys.* **107**, 074110 (2010).
- ¹⁸A.-M. Welsch, B. Mihailova, M. Gospodiv, R. Stosch, B. Gutter, and U. Bosmayer, *J. Phys. Cond. Matt.* **21**, 235901 (2009).
- ¹⁹V. J. Tennery, K. W. Hang, and R. E. Novak, *J. Am. Ceram. Soc.* **51**, 671 (1968).
- ²⁰R. Haumont, A. Al-Barakaty, B. Dkhil, J. M. Kiat, and L. Bellaiche, *Phys. Rev. B* **71**, 104106 (2005).
- ²¹R. Haumont, B. Dkhil, J. M. Kiat, A. Al-Barakaty, H. Dammak, and L. Bellaiche, *Phys. Rev. B* **68**, 014114 (2003).
- ²²Y.-H. Bing and Z.-G. Ye, *Mater. Sci. Eng. B* **120**, 72 (2005).
- ²³Y.-H. Bing and Z.-G. Ye, *J. Cryst. Growth* **287**, 326 (2006).
- ²⁴Y.-H. Bing and Z.-G. Ye, *J. Electroceram.* **21**, 761 (2008).
- ²⁵Y. Yamashita, *Jpn. J. Appl. Phys.* **33**, 5328 (1994).
- ²⁶S. Kojima, *Jpn. J. Appl. Phys.* **49**, 07HA01 (2010).
- ²⁷W. Rie and X. Ren, *Phys. Rev. Lett.* **103**, 257602 (2009).
- ²⁸I. G. Siny, S. G. Lushnikov, R. Katiyar, and E. A. Rogacheva, *Phys. Rev. B* **56**, 7962 (1997).
- ²⁹W. Hayes and W. Loudon, *Scattering of Light by Crystals* (Dover, New York, 1978).
- ³⁰V. Sivasubramanian, S. Tsukada, and S. Kojima, *J. Appl. Phys.* **105**, 014108 (2009).
- ³¹M. E. Lines and A. M. Glass, *Principles and Applications of Ferroelectrics and Related Materials* (Oxford Press, Oxford, 1977).
- ³²J.-H. Ko, D. H. Kim, S. Tsukada, S. Kojima, A. A. Bokov, and Z.-G. Ye, *Phys. Rev. B* **82**, 104110 (2010).
- ³³K. Trachenko and V. V. Brazhkin, *J. Phys.: Condens. Matter.* **21**, 425104 (2009).
- ³⁴G. Adam and J. H. Gibbs, *J. Chem. Phys.* **43**, 139 (1939).
- ³⁵G. Xu, J. Wen, C. Stock, and R. M. Gehring, *Nature Mater.* **7**, 562 (2008).
- ³⁶S. Kojima and S. Tsukada, *Ferroelectrics*, **405**, 32 (2010).